encit 2020

ABCM Associação Brasileira de Engenharia e Ciências Mecânicas

18th Brazilian Congress of Thermal Sciences and Engineering
November 16–20, 2020 (Online)

# ENC-2020-0653
# DYNAMICS OF FLUIDS PERMEATION AND SOLUTE TRANSPORT IN A SPHERICAL POLYMER GEL

**Natanaele S. Medeiros**
**Francisco S. Forte Neto**
**Antônio G. B. da Cruz**
Faculdade de Engenharia Mecânica/ITEC, Universidade Federal do Pará
aguicruz@ufpa.br

**Fernando P. Duda**
Programa de Engenharia Mecânica, COPPE/UFRJ, Rio de Janeiro, Brazil
duda@mecanica.coppe.ufrj.br

***Abstract.*** *In this paper, we consider a finite-strain theory for solute transport in polymer gels. With this modeling approach, we emphasize the main underlying phenomena of fluids permeation in a spherical gel immersed in a fluid bath through a numerical study. Besides the large deformation, we describe the volume changes of the gel and the amount of solute with various elasticity moduli as functions of swelling and deswelling time in the fluid bath.*

***Keywords:*** *hydrogels, diffusion, large deformation, fluid permeation, finite-elements*

## 1. INTRODUCTION

Stimuli-responsive properties of polymer gels account for the growing interest surrounding them, including their responsiveness to different chemo-physical environment stimuli such as pH, temperature, and humidity; polymer gels react to these stimuli by varying their fluid content through swelling–deswelling mechanisms, as observed in Fried and Puntel (2020). In the particular field of polymer gels for delivery of bioactive agents, it was shown that in drug release systems using hydrogels as drug carriers, the presence of the polymer network reduces the drug release rate, which can extend the release period (Xu *et al.*, 2013). According to Liu *et al.* (2017), controlled drug release systems can reduce the dosing frequency to relieve the pain of the patients, strengthen the drug efficacy and reduce the side effects. Besides, Ninawe and Parulekar (2012) found that the ability of drug molecules to diffuse into and out of hydrogels allows the use of these as drug delivery systems for various routes of administration. Swelling and deswelling mechanisms involve a moving boundary owing to the displacement of polymer network of the hydrogel, which in turn influences interstitial space network, permeability, and transport of drug and fluid in polymer gels (Ninawe and Parulekar, 2012). A chemomechanical model for changes of volume, shape, permeation, and mechanical properties in responsive hydrogels that accounts for the competing time scales associated with the transport of solute molecules will play a pivotal role in advancing drug delivery and solute transport in medicine.

With this in mind, in this paper, we consider a finite-strain theory for solute transport in polymer gels. Our main purpose is to investigate the dynamics of fluid permeation and the large deformation undergone by the gel in the solute transport. The theory couples mass diffusion and large deformation in polymer gels for predicting solute loading into gels from a well-mixed solution and solute release from gel into a target fluid environment. The model is simplified to study fluids permeation and solute transport in a spherical gel under swelling and deswelling behaviors. The full model was implemented in a one-dimensional symmetric sphere through a weak formulation and solved using a mixed finite element method in the platform FEniCS. This simple problem generates several non-trivial insights into the dynamics of fluids permeation and solute transport in polymer gels.

The outline of this paper is as follows. In Section 2, we introduce the finite-strain theory for solute transport and large deformation. In Section 3, we discuss the variational formulation of the finite-strain theory and numerical details of implementation in FEniCS. In Section 4, we discuss the results of dynamic behavior and solute transport in a spherical gel under swelling and deswelling processes. We conclude and present our outlook for future research in Section 5.

## 2. THEORETICAL MODEL

In this work, we adopted a modified version of the nonlinear theory for diffusion and large deformation in polymer gels introduced by Duda *et al.* (2010). The theory considers that the elastic solid represented by the polymer network

undergoes two interdependent processes at different scales, namely, a macroscopic or mechanical process due to the large elastic deformation of the network and microscopic or chemical processes due to the fluid permeation through the network and solute transport within the fluid. In the reference non-deformed configuration, $\mathcal{B}$ denotes the elastic solid matrix in a stress-free and capable to absorbs a interstitial fluid. The kinematic representation involves the following fields. We define the deformation mapping of the material point $\mathbf{X}$ in the reference (non-deformed configuration) space into a spatial point $\mathbf{x}$ in the physical space (deformed configuration) by the time-dependent transformation $\mathbf{y}(\mathbf{X},t)$. The displacement field is $\mathbf{u}(\mathbf{X},t)=\mathbf{x}-\mathbf{X}$. The deformation of the network is characterized by the deformation gradient tensor $\mathbf{F}=\nabla\mathbf{y}=\mathbf{I}+\nabla\mathbf{u}$. The fluid concentration is $c(\mathbf{X},t)$ and solute concentration is $c_s(\mathbf{X},t)$ in time $t$. Besides, we assume that the permeation of fluids under mechanical loads must satisfy the constraint $\det\mathbf{F}=1+\upsilon c$, where $\upsilon$ denotes the volume occupied by one molecule of fluid, and represents the classical restriction that solid matrix and fluid are both incompressible.

Let $\mathbf{S}(\mathbf{X},t)$ denote the Piola stress tensor. Denote by $\mathrm{Div}$ the divergent operator in $\mathcal{B}$ and the material time derivative by a superposed dot. When inertia is neglected, which is reasonable in applications involving the use of polymer gels, the mechanical and chemical balances require that

$$\mathrm{Div}\,\mathbf{S}=\mathbf{0},\qquad \frac{1}{\upsilon}\dot{\det\mathbf{F}}=-\mathrm{Div}\,\mathbf{J},\qquad \text{and}\qquad \dot{c}_s=-\mathrm{Div}\mathbf{J}_s, \tag{1}$$

with the constitutive responses given by

$$\left.\begin{aligned}
\mathbf{S}&=\mathbf{S}_n-p\mathbf{F}^*,\\
\mathbf{S}_n&=nk_BT\mathbf{F}-\Pi\mathbf{F}^*,\\
\Pi=-\frac{k_BT}{\upsilon}\left(\ln\left(\frac{\det\mathbf{F}-1}{\det\mathbf{F}}\right)+\frac{1}{\det\mathbf{F}}+\frac{\chi}{(\det\mathbf{F})^2}\right)&+\frac{k_BT}{\upsilon}\left(\frac{c_s}{(\det\mathbf{F}-1)/\upsilon}\right),\\
\mathbf{J}&=-\frac{D(\det\mathbf{F}-1)}{k_BT}\left(\mathbf{F}^\top\mathbf{F}\right)^{-1}\nabla p,\\
\mathbf{J}_s&=\mathbf{J}_s^f+\frac{\mathbf{J}}{c}c_s,\\
\mathbf{J}_s^f&=-\frac{D_sc_s}{k_BT}\left(\mathbf{F}^\top\mathbf{F}\right)^{-1}\nabla\mu_s,\\
\mu_s&=\mu_s^0+k_BT\left(\ln\frac{c_s}{c}\right).
\end{aligned}\right\} \tag{2}$$

The specialized theory in Eqs. (1)-(2) is defined in terms of the cross-linked units per volume of reference $n$, the volume of one fluid molecule $\upsilon$, and Flory-Huggins parameter $\chi$ that characterizes the interactions between fluid and polymeric network. In Eq. $(2)_1$, $nk_BT$ represents the elastic modulus of the network, where $k_B$ is the Boltzmann constant and $T$ absolute temperature. $\mathbf{S}_n$ represents the local tension in the polymeric network, $\pi$ is the osmotic pressure, $\mathbf{F}^*=(\det\mathbf{F})\mathbf{F}^{-\top}$, and $\mu_s$ is the chemical potential of the solute species. Importantly, we used the incompressibility constraint of the mixture to write the fluid concentration as $c=(\det\mathbf{F}-1)/\upsilon$. Further, the model assumes the dissipation processes involved are only associated with the fluid flow relative to the solid network, $\mathbf{J}$, and solute species flow relative to the fluid, $\mathbf{J}_s^f$. In Eq. $(2)_1$, the total Piola stress $\mathbf{S}$ is given by the sum of two contributions, one due to the network $\mathbf{S}_n$ and other due to the interstitial fluid $p\mathbf{F}^*$. The network stress in turn comes from two contributions, one elastic and other osmotic. The same holds for the total Cauchy stress tensor $\mathbf{T}=(\det\mathbf{F})^{-1}\mathbf{S}\mathbf{F}^\top$ in the physical deformed configuration. The network contributions arise from the elastic free energy of the gel and the osmotic pressure, see Duda *et al.* (2010). Note that, for a dry material point, $p$ corresponds to the standard pressure that appears due to incompressibility.

The treatment of the boundary conditions for the mechano-chemical problem defined in Eqs. (1)-(2) is standard. The mechanical environment involves the prescription of either $\mathbf{u}$ or $\mathbf{S}\mathbf{n}=(\mathbf{S}_n-p\mathbf{F}^*)\mathbf{n}$ for $(1)_1$, whereas conditions for Eq. $(1)_2$ involve the prescription of either environmental pressure $p$ or $\mathbf{n}\cdot\mathbf{J}$, and conditions for Eq. $(1)_3$ involve prescribing either the solute concentration $c_s$ or the flux $\mathbf{n}\cdot\mathbf{J}_s=\mathbf{n}\cdot\left(\mathbf{J}_s^f+\frac{\mathbf{J}}{c}c_s\right)$.

### 2.1 Spherical hydrogel

We applied the theoretical model presented above to study a one-dimensional problem of swelling and deswelling spherical hydrogel into a target fluid. We consider a situation that $\mathcal{B}$ is identified with a spherical region of radius $A$, given by

$$\mathcal{B}:=\{(R,\Theta,\Phi)|\,0\le R\le A,\,0\le\Theta\le2\pi,\,0\le\Phi\le\pi\}, \tag{3}$$

where a material point $\mathbf{X}=(R,\Theta,\Phi)$ in $\mathcal{B}$ is mapped by the motion $\mathbf{y}(\mathbf{X},t)$ to occupy the position $\mathbf{x}=(r,\theta,\phi)$ in the deformed configuration. By assuming spherical symmetry in which the displacement field, fluid content, and solute

species concentration depend at most on radial position $R$ and time $t$, yields

$$\mathbf{u} = u(R,t)\mathbf{e}, \quad c = c(R,t) \quad \text{and} \quad c_s = c_s(R,t), \tag{4}$$

where $\mathbf{e}$ represents the unit vector along the radial direction. Under this assumption, the mapping from the reference into the deformed configuration is taken to have the form

$$r(R,t) = R + u(R,t), \quad \theta = \Theta \quad \text{and} \quad \phi = \Phi, \tag{5}$$

where the field displacement $u$ obeys $u(0,t) = 0$. The deformation gradient tensor $\mathbf{F}$ in matrix representation is $[\mathbf{F}] = \mathrm{diag}\{\lambda_R, \lambda, \lambda\}$, where $\lambda_R = \frac{\partial r(R,t)}{\partial R}$ is the radial stretch and $\lambda = \frac{r(R,t)}{R}$ is the circumferential stretch. This imply that the stress tensor $\mathbf{S}$ has the following matrix representation:

$$[\mathbf{S}] = \mathrm{diag}\left\{S_{n_{RR}} - p\lambda^2, S_n - p\lambda_R\lambda, S_n - p\lambda_R\lambda\right\}, \tag{6}$$

where $S_{n_{RR}} = nk_BT\lambda_R - \Pi\lambda^2$ is the radial network stress component and $S_n = nk_BT\lambda - \Pi\lambda_R\lambda$ is the circumferential network stress component. The osmotic pressure is given by

$$\Pi = -\frac{k_BT}{\upsilon}\left(\ln\left(\frac{1-J}{J}\right) + \frac{1}{J} + \frac{\chi}{J^2}\right) + \frac{k_BT}{\upsilon}\frac{c_s}{c}, \tag{7}$$

defined in terms of the swelling ration $J = \det\mathbf{F} = \lambda_R\lambda^2$.

The initial-boundary value problem governing the fluid permeation in the spherical hydrogel is

$$\frac{\partial S_{RR}}{\partial R} + \frac{2(S_{RR} - S_{\Theta\Theta})}{R} = 0, \quad \frac{1}{\upsilon}\overline{\dot{\lambda}_R\lambda^2} = -\frac{1}{R^2}\frac{\partial}{\partial R}\left(R^2J_R\right), \quad \dot{c}_s = -\frac{1}{R^2}\frac{\partial}{\partial R}\left(R^2J_{s_R}\right) \tag{8}$$

where $S_{RR}$ and $S_{\Theta\Theta}$ represents the radial and circumferential components of the stress tensor (6), and $J_{s_R} = \left(J^f_{s_R} + \frac{J_R}{c}c_s\right)$. The radial flux components $J_R$ and $J^f_{s_R}$ are

$$J_R(R,t) = -\frac{D(\lambda_R\lambda^2 - 1)}{k_BT}\frac{1}{\lambda_R^2}\frac{\partial p}{\partial R} \quad \text{and} \quad J^f_{s_R}(R,t) = -\frac{D_sc_s}{k_BT}\frac{1}{\lambda_R^2}\frac{\partial \mu_s}{\partial R}. \tag{9}$$

Boundary conditions specialized to the spherical problem yields $u = 0$ and null fluxes $n_RJ_R = 0$ and $n_RJ_{s_R} = 0$ at $R = 0$. We set $S_{RR}n_R = 0$, $p = p_a$, and prescription of the solute concentration $c_{s_a}$ at $R = A$. In addition, we consider a initial situation in which the gel is at equilibrium and stress-free with swelling ration $\lambda_0$. Therefore, the initial conditions are settled as

$$r(R,0) = \lambda_0R, \qquad p(R,0) = p_0 \quad \text{and} \quad c_s(R,0) = c_{s_0}, \tag{10}$$

where $p_a$ is the environmental pressure and $c_{s_0}$ is the initial solute concentration. We will address this issue when setting swelling and deswelling scenarios, as shown in Figure 1.

## 3. NUMERICAL DETAILS

We implemented the spherical polymer gel model through the weak formulation of Eqs. (8) and solved using a mixed finite element method in the platform FEniCS (Alnæs *et al.*, 2015). We used an implicit Euler method to first discretize the time derivative, which yields a sequence of stationary problems, and then turn each stationary problem into a variational formulation. Thus, introducing the symbol $u$, $p$ and $c_s$ for $u^{n+1}$, $p^{n+1}$ and $c_s^{n+1}$ respectively, the resulting weak form arising from formulation Eqs. (8) can be written as: find $u$, $p$, and $c_s$, such that

$$F_{n+1}(u,p,c_s;\tilde{u},\tilde{p},\tilde{c}_s) = 0, \tag{11}$$

for any $\tilde{u}$, $\tilde{p}$, and $\tilde{c}_s$ chosen in appropriate functional spaces, where

$$\begin{aligned} F_{n+1}(u,p,c_s;\tilde{u},\tilde{p},\tilde{c}_s) = &\int_0^A\left(\frac{\partial\tilde{u}}{\partial R}S_{RR} + 2S_{\Theta\Theta}\frac{\tilde{u}}{R}\right)R^2dR + \int_0^A\left(\tilde{p}\,J - \Delta t\,\upsilon\frac{\partial\tilde{p}}{\partial R}J_R - \tilde{p}J^n\right)R^2dR \\ &+ \int_0^A\left(\tilde{c}_sc_s - \Delta t\,\frac{\partial\tilde{c}_s}{\partial R}J_{s_R} - \tilde{c}_sc_s^n\right)R^2dR. \end{aligned} \tag{12}$$

Note that the result is a sequence of spatial, stationary problems, assuming $J^n$ and $c_s^n$ is known from the previous time step. In the finite element approximation, we used quadratic shape functions for the displacement field $u$ and solute concentration $c_s$ and linear functions for interpolating pressure $p$. The mixed finite element method developed to approximate the variational formulation defined in Eq. (11), successfully resolves time-dependent and coupled mass diffusion and deformation fields, particularly at a very short-time by adopting ramping boundary conditions and damped Newton–Raphson method, as suggested in the study by Wang *et al.* (2018). Accordingly, the choice of the ramping function and $t_{\mathrm{ramp}}$ determines the smoothness of the prescribed pressure boundary conditions. It is interesting to emphasize that the results we obtained are mesh-size independent and the calculation time-step have been of order of $10^{-3}$.

## 4. RESULTS AND DISCUSSIONS

We simulate the swelling behavior of a spherical polymer gel immersed in a diluted solution until the gel reach the equilibrium, as shown in Fig. 1a. Then, we assume a deswelling process with solute releasing of the loaded spherical gel immersed in a target fluid with a lower chemical potential, as shown in Fig. 1b. For that, we extended the physical scenario studied by Curatolo *et al.* (2017) in which a spherical gel of radius $A = 1$ mm that is initially at equilibrium in almost dry conditions, with stretch $\lambda_0 \simeq 1.006$, corresponding to a chemical potential $\mu_0 \simeq -6500$ J/mol obtained with air of relative humidity 0.07 and $c_0 = 1006$ mol/m$^3$. Here, we assume that the sphere of gel is immersed in a diluted solution at $\mu_a \simeq 0$, it swell until a new equilibrium state is reached, with radius $a_I > A$. In this state, the gel is completely swollen with uniform swelling ratio $\lambda^I_\infty$ and $\mu^I_\infty$. We used the following values of parameters in the numerical simulations: shear modulus of the gel $nk_BT = 50$ kPa, molar volume $\upsilon = 1.8 \times 10^{-5}$ mol/m$^3$, fluid diffusivity in the gel $D = 10^{-8}$ m$^2$/s, and enthalpy of mixing $\chi = 0.4$. Further, we assumed the diluted solution having a solute concentration $c_{s_a} = 0.01$ mol/m$^3$ with solute diffusion coefficient in the fluid $D_s = 2.895 \times 10^{-11}$ m$^2$/s (Ninawe and Parulekar, 2012). With these choice values, the swollen equilibrium state is characterized by $\lambda^I_\infty \simeq 3.13$ and $c^I_{s_\infty} \simeq 0.01$ mol/m$^3$. Then, when the swollen spherical gel is immersed in a pure solvent at $\mu_a = -10$ J/mol and zero solute, $c_{s_0} = 0$, it deswells until a new spherical equilibrium state is reached having radius $a^{II}$, with $A < a^{II} < a^I$. After releasing all the solute content and part of the solvent concentration to the target fluid, the steady deswollen state is characterized by $\lambda^{II}_\infty \simeq 1.83$ and $c^{II}_{s_\infty} = 0$.

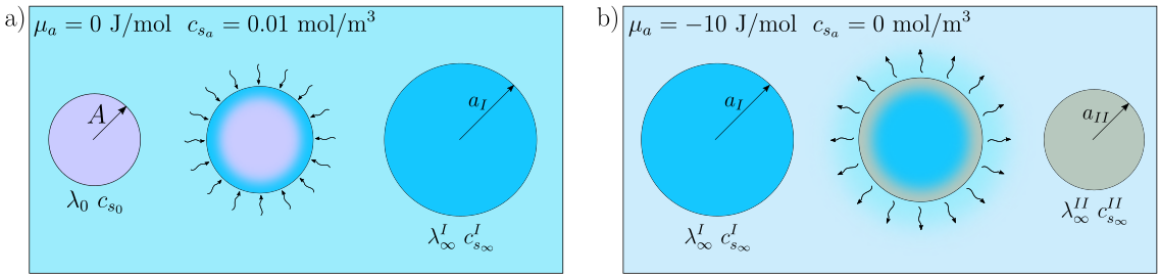


Figure 1. (a) schematic of the swelling with solute loading and (b) deswelling with solute releasing.

We have seen that considering a ramping time $t_{\text{ramp}} = \frac{t_{\text{ch}}}{10}$, the finite elements simulation agrees very well with the benchmark solution found in the studies by Curatolo *et al.* (2017) from very short time (i.e., $t = t_{\text{ch}}$), where the characteristic time scale $t_{\text{ch}} = L^2/D$; $L$ is the characteristic size of the spherical gel. Figure 2 shows the dimensionless radial and hoop stretching rates $\lambda_R$ and $\lambda$ respectively, at a point on the outer surface of the gel sphere in the deformed configuration that is evolving in time for both swelling and deswelling behaviors. We observed that the radial and hoop stretches rates are larger than 1 on the outer surface for the swelling behavior, driving the swelling growth of the gel sphere (Fig. 2a). Similar behavior is found in the studies by Curatolo *et al.* (2017). We observe that radial stretch rate $\lambda_R$ is below to the hoop stretches rate $\lambda$ as deswelling behavior evolves in time and presents values lower than 1 (Fig. 2b). It is interesting to note, however, that $\lambda_R$ rapidly decreases in early times and assumes values lower than 1 as the deswelling behavior occurs faster than swelling. Further, it suggests that the relaxation of the network stress in the polymer gel accelerates the deswelling process and assists to squeeze the fluid out of the gel.

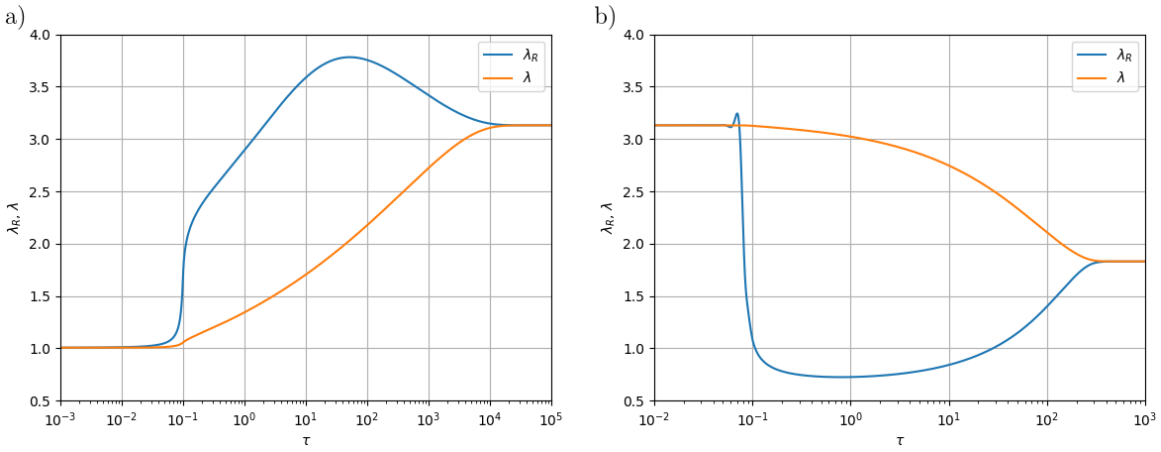


Figure 2. Time evolution of the radial $\lambda_R$ and hoop $\lambda$ stretching rates for (a) swelling and (b) deswelling at a point on the outer surface of the gel sphere.

Figure 3 shows the dimensionless radial and hoop stress $\sigma_{rr}/nk_BT$ and $\sigma_{\theta\theta}/nk_BT$ respectively, at a point on the outer surface of the gel sphere in the physical deformed configuration that is evolving in time. For the swelling behavior (Fig. 3a), the radial and hoop stresses are present positive tensile as the elastic network are being stretched to accommodate the fluid absorbed by the gel. As commonly observed in spherical gel, the rapid swelling on the outer region is restrained by the unswollen core driving to the strong radial stress that relaxes as the swelling proceeds toward the gel sphere. It is interesting to note that on the surface of the gel, $\sigma_{rr}/nk_BT$ increases fast from the initial value 1 at around $\tau = 10^{-2}$, remaining greater than $\sigma_{\theta\theta}/nk_BT$ during the entire swelling process until the homogeneous equilibrium state is reached at $\tau = 10^4$. Here, $\sigma_{rr}/nk_BT$ represents the mechanical contribution to chemical potential $\mu$ that is the driving force of the swelling process, as observed in Curatolo *et al.* (2017). For the deswelling process (Fig. 3b), the radial and hoop stresses remain tensile, and the polymeric network is in intense hoop stress because the fluid is being squeezed out of the gel sphere by the tight and contracting the outer region, on the contrary of the swelling process. Note that the radial stress decreases, whereas hoop stress rapidly increases in early times. However, once the drying front arrives at the center of the gel sphere, these stresses smoothly go toward their final equilibrium values.

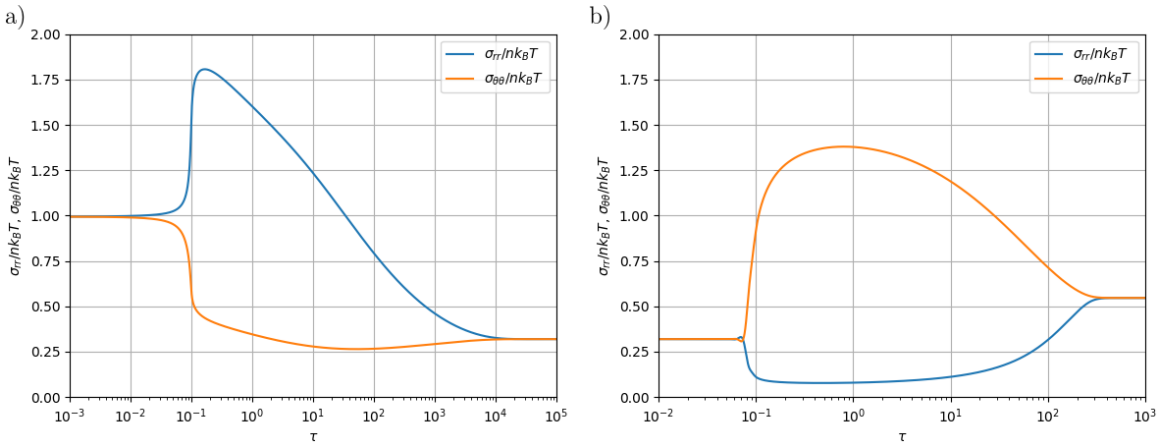


Figure 3. Time evolution of the radial and hoop stresses at a point on the outer surface of the gel sphere for (a) swelling and (b) deswelling process.

Figure 4 shows the volume changes of the spherical gel for different modulus of elasticity $nk_BT$ as a function of the swelling time in solution. The fluid absorption capacity of the gel sphere changes with the modulus of elasticity $nk_BT$ values that in turn change with the number of cross-links $n$ of the polymeric network. It is interesting to note that the more elastic is the network (i.e., low value of $nk_BT$), the greater the quantity of fluid permeation and the larger the swelling (Fig. 4a). We observe a similar behavior for the fluid release in the deswelling process (Fig. 4b).

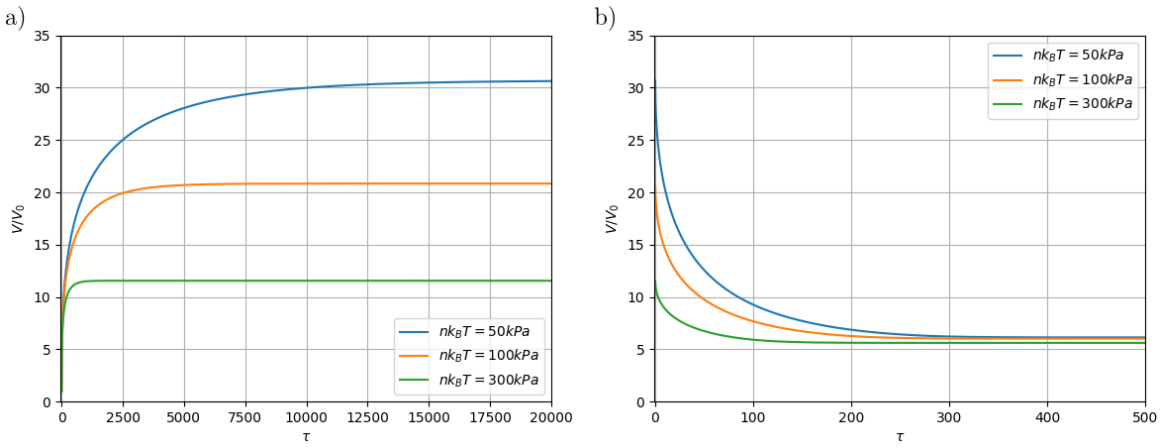


Figure 4. Volume changes of the gel sphere as functions of swelling (a) and deswelling (b) time.

Figure 5 shows the amount of solute loaded and released by the gel for different modulus of elasticity $nk_BT$ as a function of the swelling time in solution. The amount of solute in the gel sphere related to the undeformed configuration is obtained by

$$m_s(t) = 4\pi \int_0^A c_s(R,t) J R^2 dR \tag{13}$$

and $m_\infty$ represents the value of the solute amount in gel sphere at the equilibrium for $nk_BT = 50$ kPa. Note that the permeation and releasing capability of the spherical gel strongly change with the elasticity of the network, where for greater values of the modulus of elasticity we have a small amount of solute loaded and released by the sphere gel. However, for lower values of the elastic modulus, the sphere gel undergoes a greater volume change (Fig. 5a), and consequently greater is the amount of solute loaded or released by the gel (Fig. 5b).

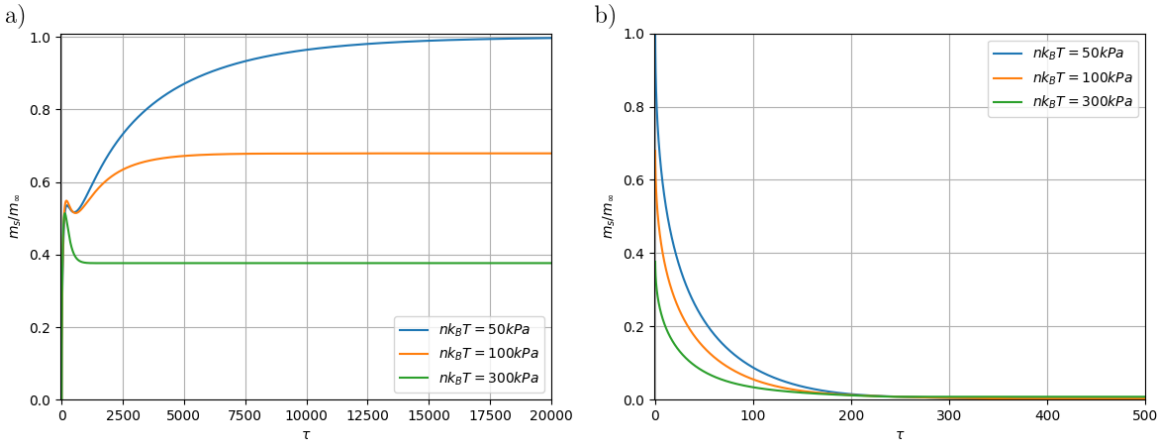


Figure 5. Evolution of the amount of solute loaded (a) and released (b) by the gel sphere as functions of swelling and deswelling dimensionless time.

## 5. CONCLUDING REMARKS

In this work, we investigated the swelling and deswelling dynamics driven by fluid permeation and solute transport in a polymer gel sphere immersed in a target fluid. For analyze, we adopted a finite-strain theory for solute transport in polymer gels. We described the evolution of the polymer gel deformation, amount of the solute, and volume changes of the gel sphere with various elasticity moduli as functions of swelling and deswelling time in a target fluid. The study provides insight into quantities that are difficult to measure in experiments, such as the volume changes and the amount of solute transport in swelling and deswelling of the polymer gel. Future analysis will be conducted on appropriate physical scenarios for a deep investigation of the role played by the large deformation undergone by the gel in the solute transport.

## 6. ACKNOWLEDGEMENTS

The authors acknowledge the Coordenação de Aperfeiçoamento de Pessoal de Nível Superior–CAPES for support (Finance Code: 88881.200549/2018-01).

## REFERENCES

Alnæs, M.S., Blechta, J., Hake, J., Johansson, A., Kehlet, B., Logg, A., Richardson, C., Ring, J., Rognes, M.E. and Wells, G.N., 2015. "The fenics project version 1.5". *Archive of Numerical Software*, Vol. 3, No. 100. doi: 10.11588/ans.2015.100.20553.

Curatolo, M., Nardinocchi, P., Puntel, E. and Teresi, L., 2017. "Transient instabilities in swelling dynamics". *arXiv preprint arXiv:1704.08201*.

Duda, F.P., Souza, A.C. and Fried, E., 2010. "A theory for species migration in a finitely strained solid with application to polymer network swelling". *Journal of the Mechanics and Physics of Solids*, Vol. 58, No. 4, pp. 515–529.

Fried, E. and Puntel, E., 2020. "Thematic issue of mechanics of materials: Mechanics, chemistry, and thermodynamics of gels".

Liu, Y., Ye, H. and Jia, Y., 2017. "Finite element simulation of swelling and drug release processes using weak polyelectrolyte hydrogels as drug carrier". *Journal of Controlled Release*, Vol. 259, pp. e186–e187.

Ninawe, P.R. and Parulekar, S.J., 2012. "Drug delivery using stimuli-responsive polymer gel spheres". *Industrial & engineering chemistry research*, Vol. 51, No. 4, pp. 1741–1755.

Wang, X., Zhai, Z., Chen, Y. and Jiang, H., 2018. "A facile, robust and versatile finite element implementation to study the time-dependent behaviors of responsive gels". *Extreme Mechanics Letters*, Vol. 22, pp. 89–97.

Xu, Y., Jia, Y., Wang, Z. and Wang, Z., 2013. "Mathematical modeling and finite element simulation of slow release of drugs using hydrogels as carriers with various drug concentration distributions". *Journal of pharmaceutical sciences*, Vol. 102, No. 5, pp. 1532–1543.

## 7. RESPONSIBILITY NOTICE

The authors are solely responsible for the printed material included in this paper.